

Article

The Robust Emergency Medical Facilities Location-Allocation Models under Uncertain Environment: A Hybrid Approach

Fang Xu ¹, Mengfan Yan ², Lun Wang ^{2,3,*} and Shaojian Qu ⁴ ¹ Sino-German College, University of Shanghai for Science and Technology, Shanghai 200093, China² Business School, University of Shanghai for Science and Technology, Shanghai 200093, China³ School of Management, Shanghai University, Shanghai 200444, China⁴ School of Management Science and Engineering, Nanjing University of Information Science and Technology, Nanjing 210044, China

* Correspondence: 203781404@st.usst.edu.cn

Abstract: In emergency medical facilities location, the hierarchical diagnosis and treatment system plays an obvious role in the rational allocation of medical resources and improving the use efficiency of medical resources. However, few studies have investigated the operational mechanism of hierarchical medical systems in uncertain environments. To address this research gap, this paper proposes a hybrid approach for emergency medical facilities' location-allocation. In the first stage, in order to concentrate on the utilization of medical resources, we choose alternative facility points from the whole facilities through the entropy weight method (EWM). In the second stage, uncertainty sets are used to describe the uncertain number of patients at emergency medical points more accurately. We propose a robust model to configure large base hospitals based on the robust optimization method. Furthermore, the proposed robust models are applied to the emergency management of Huanggang City under COVID-19. The results show that the optimal emergency medical facility location-allocation scheme meets the actual treatment needs. Simultaneously, the disturbance ratio and uncertainty level have a significant impact on the configuration scheme.

Keywords: emergency medical facilities; entropy weight method; robust optimization; location-allocation; hierarchical diagnosis and treatment system



Citation: Xu, F.; Yan, M.; Wang, L.; Qu, S. The Robust Emergency Medical Facilities Location-Allocation Models under Uncertain Environment: A Hybrid Approach. *Sustainability* **2023**, *15*, 624. <https://doi.org/10.3390/su15010624>

Academic Editors: Mark A. Bonn and Ting Chi

Received: 2 November 2022

Revised: 11 December 2022

Accepted: 26 December 2022

Published: 29 December 2022



Copyright: © 2022 by the authors. Licensee MDPI, Basel, Switzerland. This article is an open access article distributed under the terms and conditions of the Creative Commons Attribution (CC BY) license (<https://creativecommons.org/licenses/by/4.0/>).

1. Introduction

Public health emergencies such as COVID-19 have brought great threats to people and society [1–5]. For timely responses, a hierarchical diagnosis and treatment mode should be established to isolate, control, and treat patients [6–12]. During the epidemic period, the hierarchical diagnosis and treatment mode [13,14] avoided the paralysis of large hospitals caused by the concentration of a large number of patients, and the use efficiency of medical resources was significantly improved. At the same time, medical resources have been reasonably allocated [15]. It is crucial to improve residents' satisfaction and happiness [16].

At present, many scholars have investigated facility location problems [17]. Biswas and Pamucar [18] studied the factors affecting the school location decision from the perspective of students. They developed an integrated group decision-making framework, that is, a pivot pairwise relative criteria importance assessment (PIPRECIA). Pamucar et al. [19] conducted location selection for wind farms using a GIS multi-criteria hybrid model based on fuzzy and rough numbers. Boonmee et al. [20] summarized the humanitarian facility location problem. They divided the location problem into a deterministic facility location problem, dynamic facility location problem, stochastic facility location problem, and robust facility location problem, respectively. Deterministic facility location problems form the basis for dynamic, stochastic, and robust models. However, the medical facility location problem is facing more and more uncertainties (e.g., the uncertain number of patients in facility points, the uncertainty of transportation costs, etc.). The deterministic facility

location model cannot describe the impact that uncertain parameter changes have on the facility location problem, which has a certain gap with the actual situation. Therefore, the deterministic facility location model has some disadvantages. Stochastic, dynamic, and robust facility location models can be used to respond to real situations. The dynamic programming model is effective for solving multi-stage decision problems. However, the calculation amount of the dynamic facility location problem increases dramatically when the dimension of decision variables increases. Today's computers still cannot effectively solve large-scale dynamic facility location problems in actual emergency medical responses. For the stochastic facility location, the probability distribution of random parameters needs to be precisely known in advance. In the emergency medical facilities' location, it is difficult to obtain sufficient historical data to estimate the distribution function of random parameters. In order to overcome the shortcomings of the above three methods, a robust facility location model is proposed in this paper. We take into account the uncertain number of patients at the facility points and use the uncertainty sets to describe the uncertain number of patients more accurately. Therefore, this paper focuses on the robust facility location. Extant examples of the literature have studied the emergency medical facilities' location through multi-objective programming [21], the analytic hierarchy process (AHP) and technique for order preference by similarity to an ideal solution (TOPSIS) [22], mixed integer linear programming [23,24], and so on. However, the uncertain number of patients in emergency medical sites during the epidemic situation was not taken into account in the above literature, which increased the risk of decision-making in the emergency medical facilities location and was not good for the life and health of patients. Accordingly, we need to focus on decision-making under an uncertain number of patients to reduce the uncertainty risk. On the other hand, the above-mentioned literature rarely utilized the hierarchical diagnosis and treatment system to locate the emergency medical facilities, so medical resources may not be reasonably allocated, and the use efficiency of medical resources may be reduced. Therefore, in order to deal with the impact of the epidemic more economically and effectively, the improvement of the community medical care level and the completion of the system should be the priority task, which is also beneficial to reduce the burden of large hospitals.

The robust optimization theory is widely used to deal with uncertain optimization problems. The solution of robust optimization is such that all the constraints still hold in the worst case. Unlike stochastic programming [25], robust optimization does not require the probability distribution function of the random parameters. However, it assumes that the uncertain parameters fluctuate in an interval [26–30]. Since its emergence, robust optimization theories have been applied to many fields, such as group decision-making [31–36], portfolios [37–41], efficiency evaluation [42,43], supply chain management [44–49], etc. In emergency medical location decisions, some scholars have adopted the stochastic programming method for modeling [50–54]. However, the stochastic programming needs to know the probability distribution of the patients' number at the facility point. Due to the urgency of the event, it is impossible to accurately obtain the probability function of the patient's number at the facility point. Consequently, the stochastic programming method describing the fluctuation of the patient's number has defects. Hence, in order to overcome the shortcomings of the stochastic programming, we adopted the robust optimization method to handle the uncertainty of the patients' number in the emergency medical facilities' location.

In order to effectively avoid the paralysis of large hospitals caused by the concentration of a large number of patients and to significantly improve the use efficiency of medical resources, this paper proposes a hierarchical diagnosis and treatment system for the emergency medical facilities located under the background of the epidemic. Therefore, a hybrid evaluation method, including EWM and the robust optimization method, is proposed for modeling. We have a two-step plan for post-outbreak isolation and treatment. In the first stage, 10 facilities with the highest scores are selected from 30 facilities by EWM as community emergency medical points. When there are critical patients who cannot be handled by community medical centers, the second stage of decision-making is to send the

critical patients to large base hospitals for treatment. We construct a robust location model with capacity and time window constraints with the presence of an uncertain number of patients to configure a large rear hospital.

Different from previous studies, this paper proposes a hybrid approach to cope with the emergency facilities' location problems. This approach contains two-stage decisions under a hierarchical diagnosis system. The first stage decision is to obtain reasonable alternative points from all possible facility points. The second stage decision is to optimally configure the rear hospital under uncertain demand. The contributions of this paper are as follows: Firstly, this paper studies the location-allocation of emergency medical facilities under the hierarchical diagnosis and treatment mode. A hybrid location-allocation decision for emergency medical facilities is also investigated. In the first stage, alternatives are selected from all facility points by EWM. In the second stage, considering the uncertain number of patients at emergency facility points, this paper uses uncertainty sets to describe the number of patients more accurately. On this basis, a robust model with capacity and time window constraints is constructed to allocate large base hospitals. The proposed method fully takes into account the uncertainties when the epidemic occurs. The results of location-allocation significantly reduce the risk of decision-making and provide a strong guarantee for people's health. Therefore, the optimization problem in this paper is in line with the actual situation when the epidemic occurs. Secondly, the robust optimization model is equivalently transformed into a mixed integer linear programming problem by utilizing the duality theory. The robust counterpart model can be solved in polynomial time. Finally, we conduct simulation experiments on the proposed model through the location-allocation scheme of emergency medical facilities in Huanggang City during the COVID-19 epidemic. The results verify the feasibility and robustness of the proposed model. Sensitivity analysis also shows the effectiveness of the proposed method. The proposed method of this paper can provide reference and compliance for health departments to effectively carry out regular epidemic prevention and control.

The remainder of this paper is organized as follows. Section 2 presents the framework and preliminaries; Section 3 derives the emergency facilities location modeling. Section 4 specifies numerical experiments; Section 5 concludes.

2. The Framework and Preliminaries

2.1. The Framework of This Paper

The framework of this paper is shown in Figure 1. A hierarchical diagnosis and treatment mode is proposed to cope with the impact of the pandemic. Firstly, it is unrealistic to establish emergency medical facilities at every point, considering the ease of the centralized utilization of medical resources. Hence, EWM was utilized to choose alternative facilities from the whole facilities in the first stage. Secondly, when patients at the facility points are critically ill, the robust optimization approach is used to configure the large rear hospital in the case of the uncertain number of patients in the second stage. The time window constraint is also constructed to ensure the timely treatment of patients. When patients at the facility are mild patients, they are directly isolated at the emergency medical point. Accordingly, a hybrid approach for emergency medical facilities location-allocation is proposed.

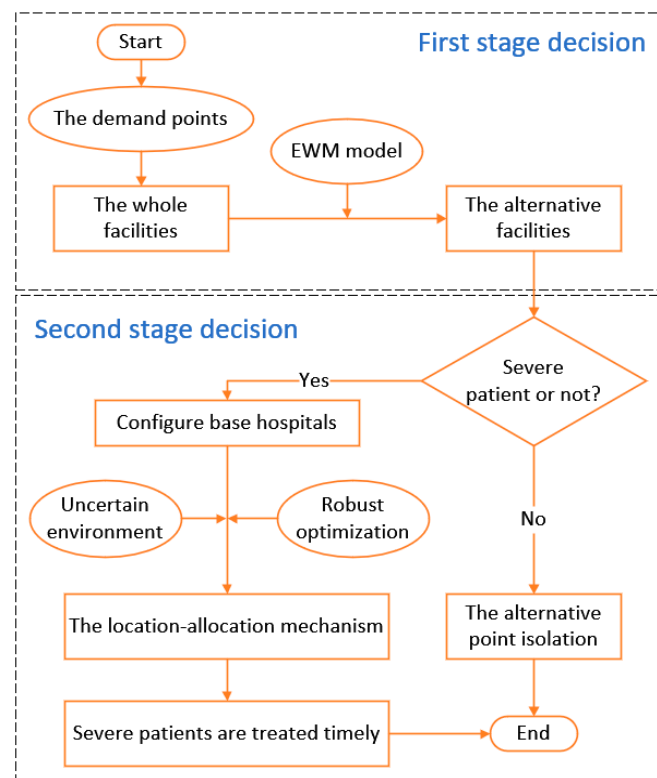


Figure 1. The resolution framework of the proposed hybrid approach.

2.2. Assumptions and Notation

In order to facilitate modeling, the following assumptions were made:

1. The established emergency medical facilities can meet the medical needs of patients in the city, regardless of the situation of transferring patients to other cities.
2. The radiation range of each facility is a small area, and the patients' number, which they receive, is the sum of the patients' number in the area.
3. All critically ill patients are treated by large rear hospitals, which do not occupy the medical resources of the facility point. Additionally, the rear hospitals can meet the treatment needs of the assigned critically ill patients.

The notation in this paper is illustrated in Table 1.

Table 1. The utilized notation in this paper.

Sets	
I	The collection of the whole emergency medical facilities (reconfigurable convention and exhibition centers, sports venues, schools), $i \in I, i = 1, 2, \dots, n$.
J	The collection of existing large rear hospitals (Grade II and above), $j \in J, j = 1, 2, \dots, m$.
K	The collection of patient types (mild, moderate, and severe three disease grades, represented by 1, 2, 3), $k \in K, k = 1, 2, 3$.
Decision variables	
x_i	$\begin{cases} 1, & \text{Open emergency medical facility point } i. \\ 0, & \text{Otherwise.} \end{cases}$
y_{ij}	$\begin{cases} 1, & \text{Patients at facility point } i \text{ are serviced by hospital } j. \\ 0, & \text{Otherwise.} \end{cases}$
z_j	$\begin{cases} 1, & \text{Select hospital } j \text{ to treat critically ill patients.} \\ 0, & \text{Otherwise.} \end{cases}$

Table 1. *Cont.*

Parameters	
S	Number of emergency medical facilities opened.
f_i	Operating cost of emergency medical facility point i .
h_{ij}	Distance from facility point i to hospital j .
c_t	Unit driving cost from facility point i to hospital j .
d_{ik}	Patients' number of k type at facility point i .
θ_k	The proportion of k type patients, respectively represents the severity level of patients.
c_j	The maximum service capacity of large rear hospital j .

3. Emergencies Facilities Location Modeling

3.1. Emergency Medical Facilities Alternatives Selection Based on EWM

In this section, we will reveal the first stage of the hybrid approach. Taking into account the ease of the centralized utilization of medical resources, it is impossible for public health departments to establish emergency medical facilities at every point. The scientific and rational decision is to select some facilities from the total of facilities as alternatives. Consequently, this paper utilizes EWM to make location decisions.

As an objective and comprehensive weighting method, EWM determines weight mainly based on the information amount transmitted to decision-makers by each index, which can effectively avoid the influence of subjective factors. Then, we can make weight calculations more scientific and reasonable. The advantages of EWM are as follows: (1) EWM can deeply reflect the ability to distinguish indicators and determine a good weight; (2) Weight assignment is more objective, theoretical, and reliable; (3) The procedure is simple and easy to practice, EWM does not require other software analysis. Therefore, the EWM method was utilized to make the first-stage decision in this paper.

The selection principles of the evaluation indicators are as follows: (1) Objective and true principles. The selected indicators should be objective and true. The data sources should be based on the official data information so as to ensure that the indicators can objectively reflect the real situation of each region and avoid deviations between the data that are caused by personal subjective assumptions and the actual situation. (2) Operability principle. Ensure that the selected index data can be obtained from statistical information released by national government departments or official media. Avoid indicators with vague information or a different statistical caliber. Additionally, we should adopt relatively easy-to-obtain and relatively stable indicator information. (3) Principle of representativeness. The selected indicators should have a certain logical relationship with each other to reflect the overall situation of each region to the greatest extent. The number of indicators should be moderate. Too many indicators will lead to high similarity, which greatly reduces computational efficiency. However, too few indicators will lead to a lack of convincing evaluation results, which is not conducive to reflecting the real situation.

According to the selection principle of evaluation indicators, this paper mainly considers three influential factors of facility location, namely cost factor, capacity factor, and infrastructure factor. Then, we constructed the evaluation index system of emergency medical locations during the epidemic situation, including the construction cost of facilities, transportation convenience, the patients' number that the facility can accommodate, regional population density, accessibility of patients, and the number of hospitals within 10 km. In terms of cost factors, due to the particularity of emergency medical facilities, this paper only considers the construction cost of facilities. Construction costs are determined according to the scale of the facility point. It is the most representative of all the cost-influencing factors. The capacity factor mainly considers the population density in the region and the number of people that can be accommodated at the facility. The capacity limit of the emergency medical point determines its maximum service capacity. The emergency treatment demand needed to be met in the administrative area to the greatest extent. As infrastructure factors, the transportation convenience degree and the accessibility of the patients are sufficient to ensure that the infected are treated and isolated in the first place

to prevent more people from becoming infected. The number of hospitals within 10 km can ensure that patients have access to transfer care and medical supplies at the large base hospital when the infected experience deterioration.

The procedure for selecting emergency medical facilities alternatives with the EWM are as follows.

Step 1: Construct the index matrix X . Let the $Y = \{y_1, y_2, \dots, y_n\}$ indicate the necessary numbers of health care providers (i.e., all the facilities points) and $A = \{a_1, a_2, \dots, a_m\}$ means the evaluation indicators. Let $I = \{1, 2, \dots, n\}$ and $J = \{1, 2, \dots, m\}$ be number sets. x_{ij} is the value of the j -th evaluation index under the facility point i , and the index matrix X is as follows:

$$X = (x_{ij})_{n \times m} = \begin{bmatrix} x_{11} & x_{12} & \cdots & x_{1m} \\ x_{21} & x_{22} & \cdots & x_{2m} \\ \vdots & \vdots & \vdots & \vdots \\ x_{n1} & x_{n2} & \cdots & x_{nm} \end{bmatrix} \quad (1)$$

Step 2: Normalize the index matrix. Since the measurement units of each index are not uniform, it is necessary to standardize them to homogenize the heterogeneous indexes. Positive indicators and negative indicators are utilized for data standardization processing. In addition, the higher the positive indicator value is, the better. Additionally, the lower the negative indicator value is, the better. The specific methods are as follows.

Positive indicators:

$$x'_{ij} = \frac{x_{ij} - \min\{x_{ij}, \dots, x_{nj}\}}{\max\{x_{1j}, \dots, x_{nj}\} - \min\{x_{1j}, \dots, x_{nj}\}} \quad (2)$$

Negative indicators:

$$x'_{ij} = \frac{\max\{x_{1j}, \dots, x_{nj}\} - x_{ij}}{\max\{x_{1j}, \dots, x_{nj}\} - \min\{x_{ij}, \dots, x_{nj}\}} \quad (3)$$

Then, the normalized index matrix is:

$$X' = (x'_{ij})_{n \times m} = \begin{bmatrix} x'_{11} & x'_{12} & \cdots & x'_{1m} \\ x'_{21} & x'_{22} & \cdots & x'_{2m} \\ \vdots & \vdots & \vdots & \vdots \\ x'_{n1} & x'_{n2} & \cdots & x'_{nm} \end{bmatrix} \quad (4)$$

Step 3: Calculate the information entropy value of the j -th index.

$$\varepsilon_j = -\frac{1}{\ln(n)} \left| \sum_{i=1}^n p_{ij} \ln(p_{ij}) \right|, j = 1, 2, \dots, m. \quad (5)$$

Here, $p_{ij} = x'_{ij} / \sum_{i=1}^n x'_{ij}$ is the proportion of the i -th emergency medical facility points under the j -th indicator when $p_{ij} = 0$, $\ln(p_{ij})$ is meaningless. In this case, the definition of p_{ij} needs to be amended, that is, $p_{ij} = (1 + x'_{ij}) / \sum_{i=1}^n (1 + x'_{ij})$.

Step 4: Calculate the entropy weight ω_j of each index.

$$\omega_j = \frac{1 - \varepsilon_j}{\left| m - \sum_{j=1}^m \varepsilon_j \right|} \quad (6)$$

Step 5: Calculate the comprehensive score s_i for each emergency medical facility point.

$$s_i = \sum_{j=1}^m \omega_j p_{ij}, i = 1, 2, \dots, n. \quad (7)$$

Therefore, if the information entropy of one index is smaller, it indicates that the variation degree of its index value is greater. The more information it provides, the greater the role it plays in the comprehensive evaluation, and the greater its weight should be. Hence, in the specific analysis process, entropy can be used to calculate the weight of each index according to the variation degree of each index value. Additionally, all the indexes are then weighted to obtain a more objective, comprehensive evaluation result.

3.2. The Deterministic Model

In this section, we allocate the large rear hospital for the alternative facility points by using the robust optimization method to ensure the timely treatment of patients in the second stage.

After a comprehensive evaluation by EWM, the alternative sites were selected. Due to limited medical conditions, emergency medical centers can only be used as a place for treating ordinary patients. When patients are seriously ill, they still need to be sent to a large rear hospital for treatment. Accordingly, we also need to configure the large rear hospitals. We should rationally allocate these emergency medical facility points to rear large hospitals through quantitative analysis. On the basis of considering the capacity limitation of base hospitals and the time window limitation of treating patients, the emergency medical facilities configuration (EMFC) model was constructed with the goal of minimizing the total cost. Thus, a complete emergency medical security system was formed that can respond to public health emergencies.

When the patients' number of k type in the emergency medical facility i is known as d_{ik} , the deterministic model (DM) is as follows:

$$\min \sum_{i \in I} f_i x_i + \sum_{i \in I} \sum_{j \in J} \sum_{k \in K} c_t h_{ij} \theta_k d_{ik} y_{ij} + \sum_{i \in I} \sum_{j \in J} p(t_{ij}) x_i \quad (8)$$

$$s.t. \sum_{i \in I} x_i \leq S \quad (9)$$

$$\sum_{j \in J} y_{ij} = 1, \forall i \in I \quad (10)$$

$$y_{ij} \leq x_i, \forall i \in I, j \in J \quad (11)$$

$$\sum_{i \in I} \sum_{k \in K} \theta_k d_{ik} y_{ij} \leq c_j, \forall j \in J \quad (12)$$

$$p(t_{ij}) = \begin{cases} 0, & 0 \leq t_{ij} < ET \\ c_p(t_{ij} - ET), & ET \leq t_{ij} < LT, \forall i \in I, j \in J \\ +\infty, & t_{ij} \geq LT \end{cases} \quad (13)$$

$$x_i \in \{0, 1\}, \forall i \in I \quad (14)$$

$$y_{ij} \in \{0, 1\}, \forall i \in I, j \in J \quad (15)$$

The objective function minimizes the total cost, which is composed of the operating cost of the emergency medical facility point, the patient transfer cost from the emergency facility point to the large rear hospital, and the penalty cost that fails to meet the optimal treatment time window.

The constraint conditions are represented from Equation (9) to Equation (15). Specifically, Equation (13) is the penalty cost function defined in this paper. The travel time t_{ij} is determined by the ratio between the distance from the facility point to the hospital

and the average speed of the transport vehicle, i.e., $(t_{ij} = h_{ij} / \bar{v}_j, \forall i \in I, j \in J)$. When the patient's condition becomes worse, the optimal treatment time is ET and the recoverable time window is $[ET, LT]$. When $0 \leq t_{ij} < ET$, the patient can arrive at the base hospital for treatment with no penalty cost, i.e., $(p(t_{ij}) = 0)$. When the patient arrives in the time window $[ET, LT]$, a punishment cost $c_p(t_{ij} - ET)$ is generated. Additionally, $p(t_{ij})$ will increase with the increase in the arrival time. Once the patient's arrival time exceeds the latest recoverable time LT , the patient's life safety is endangered, and the cost increases infinitely.

In addition, Equation (9) represents the maximum number of opened emergency medical facility points. Equation (10) indicates that each emergency medical facility point is serviced by one large rear hospital and can only be served by one rear hospital. Equation (11) means that patients can be sent to the rear hospital for treatment only when the emergency medical facilities have opened. Equation (12) indicates that the number of patients sent from the emergency facility point to the large rear hospital does not exceed the maximum service capacity of the hospital. Equation (14) and Equation (15) are both a 0–1 integer decision variable.

3.3. The Robust Model

When a public health emergency occurs, the number of patients is highly uncertain. Therefore, this paper draws on the robust decision idea of Bertsimas and Sim; we adopted the absolute robust criterion to optimize the target from the worst case [30]. Specifically, we used \tilde{d}_{ik} to represent the patients' number of k type in the emergency medical facility point i under uncertain circumstances. Then, we had $\tilde{d}_{ik} \subseteq [d_{ik} - \hat{d}_{ik}\xi_{ik}, d_{ik} + \hat{d}_{ik}\xi_{ik}]$, where d_{ik} is the nominal value and \hat{d}_{ik} is its disturbance value.

Under the disturbance of uncertain parameters, the original deterministic model can be equivalently transformed into the following robust optimization (RM) model:

$$\begin{aligned} & \min \left\{ \sum_{i \in I} f_i x_i + \max_{\xi \in U^p} \sum_{i \in I} \sum_{j \in J} \sum_{k \in K} c_t h_{ij} \theta_k (d_{ik} + \hat{d}_{ik} \xi_{ik}) y_{ij} + \sum_{i \in I} \sum_{j \in J} p(t_{ij}) x_i \right\} \\ & = \min \left\{ \sum_{i \in I} f_i x_i + \sum_{i \in I} \sum_{j \in J} \sum_{k \in K} c_t h_{ij} \theta_k d_{ik} y_{ij} + \sum_{i \in I} \sum_{j \in J} p(t_{ij}) x_i \right. \\ & \quad \left. + \max_{\xi \in U^p} \sum_{i \in I} \sum_{j \in J} \sum_{k \in K} c_t h_{ij} \theta_k \hat{d}_{ik} \xi_{ik} y_{ij} \right\} \end{aligned} \quad (16)$$

$$\text{s.t. (9) } \sim (11), (13) \sim (15)$$

$$\sum_{i \in I} \sum_{k \in K} \theta_k d_{ik} y_{ij} + \max_{\xi \in U^p} \sum_{i \in I} \sum_{k \in K} \theta_k \hat{d}_{ik} \xi_{ik} y_{ij} \leq c_j, \forall j \in J \quad (17)$$

Here, Equation (16) minimizes the total cost of the system in the worst case. Equation (17) indicates that the number of patients transported from the emergency medical facility point to the base hospital cannot exceed the maximum service capacity of the hospital in the worst case. In order to further specify the proposed robust model, three models based on different uncertainty sets were introduced as follows.

3.3.1. Budgeted Uncertainty Set

Proposition 1. *If the uncertain patients' number is defined as a budgeted uncertainty set, that is, $U^p = \left\{ \xi : \sum_{i \in I} \xi_{ik} \leq \Gamma_k, 0 \leq \xi_{ik} \leq 1, \forall k \in K \right\}$, we can obtain the following robust equivalent model (REM):*

$$\min \sum_{i \in I} f_i x_i + \sum_{i \in I} \sum_{j \in J} \sum_{k \in K} c_t h_{ij} \theta_k d_{ik} y_{ij} + \sum_{i \in I} \sum_{j \in J} p(t_{ij}) x_i + \eta \quad (18)$$

$$s.t. \eta \geq \sum_{i \in I} \sum_{k \in K} u_{ik} + \sum_{k \in K} v_k \Gamma_k \quad (19)$$

$$u_{ik} + v_k \geq c_t h_{ij} \theta_k \hat{d}_{ik} y_{ij}, \forall i \in I, j \in J, k \in K \quad (20)$$

$$u_{ik}, v_k \geq 0, \forall i \in I, k \in K \quad (21)$$

$$\sum_{i \in I} x_i \leq S \quad (22)$$

$$\sum_{j \in J} y_{ij} = 1, \forall i \in I \quad (23)$$

$$y_{ij} \leq x_i, \forall i \in I, j \in J \quad (24)$$

$$\sum_{i \in I} \sum_{k \in K} \theta_k d_{ik} y_{ij} + \sum_{i \in I} \sum_{k \in K} u'_{ik} + \sum_{k \in K} v'_k \Gamma_k \leq c_j, \forall j \in J \quad (25)$$

$$u'_{ik} + v'_k \geq \theta_k \hat{d}_{ik} y_{ij}, \forall i \in I, j \in J, k \in K \quad (26)$$

$$u'_{ik}, v'_k \geq 0, \forall i \in I, k \in K \quad (27)$$

$$p(t_{ij}) = \begin{cases} 0, & 0 \leq t_{ij} < ET \\ c_p(t_{ij} - ET), & ET \leq t_{ij} < LT, \forall i \in I, j \in J \\ +\infty, & t_{ij} \geq LT \end{cases} \quad (28)$$

$$x_i \in \{0, 1\}, \forall i \in I \quad (29)$$

$$y_{ij} \in \{0, 1\}, \forall i \in I, j \in J \quad (30)$$

Here, η is the auxiliary variable. u_{ik} and v_k are the dual variable of the problem (16). u'_{ik} and v'_k are the dual variable of the problem (17).

Proof of Proposition 1. Because the definition of the budgeted uncertainty set is

$$U^p = \left\{ \xi : \sum_{i \in I} \xi_{ik} \leq \Gamma_k, 0 \leq \xi_{ik} \leq 1, \forall k \in K \right\}, \text{ then the maximization problem}$$

$$\max_{\xi \in U^p} \left\{ \sum_{i \in I} \sum_{j \in J} \sum_{k \in K} c_t h_{ij} \theta_k \hat{d}_{ik} \xi_{ik} y_{ij} \right\} \text{ in Equation (16) is equivalent to Equation (31).}$$

$$\begin{aligned} & \max \sum_{i \in I} \sum_{j \in J} \sum_{k \in K} c_t h_{ij} \theta_k \hat{d}_{ik} \xi_{ik} y_{ij} \\ & s.t. \sum_{i \in I} \xi_{ik} \leq \Gamma_k \\ & \quad 0 \leq \xi_{ik} \leq 1 \quad \forall i \in I, k \in K \end{aligned} \quad (31)$$

According to the strong duality theory, the dual variables u_{ik} and v_k are introduced, respectively. Additionally, we can further obtain Equation (32).

$$\begin{aligned} & \min \sum_{i \in I} \sum_{k \in K} u_{ik} + \sum_{k \in K} v_k \Gamma_k \\ & s.t. u_{ik} + v_k \geq c_t h_{ij} \theta_k \hat{d}_{ik} y_{ij} \\ & \quad u_{ik}, v_k \geq 0 \quad \forall i \in I, j \in J, k \in K \end{aligned} \quad (32)$$

Hence, we can transform the inner layer maximization problem into the minimization problem, and introduce the auxiliary variable η to obtain the robust equivalent model from Equations (18)–(21).

Similarly, according to the strong duality theory, the dual variables u'_{ik} and v'_k are, respectively introduced for Equation (17), and the inner layer maximization problem is transformed into the minimization problem. Thus, Equations (25)–(27) are obtained. \square

3.3.2. Box Uncertainty Set

Proposition 2. *If the uncertain patients' number is defined as a box set, that is, $Z_{box} = \{\zeta \in R^M : \|\zeta\|_\infty \leq \psi\}$, ψ is the level of parameter uncertainty and the robust counterpart model in Section 3.3 can be constructed as follows:*

$$\begin{aligned} \min & \sum_{i \in I} f_i x_i + \sum_{i \in I} \sum_{j \in J} \sum_{k \in K} c_t h_{ij} \theta_k d_{ik} y_{ij} + \psi \sum_{i \in I} \sum_{j \in J} \sum_{k \in K} c_t h_{ij} \theta_k \hat{d}_{ik} y_{ij} + \sum_{i \in I} \sum_{j \in J} p(t_{ij}) x_i \\ \text{s.t.} & \sum_{i \in I} x_i \leq S \\ & \sum_{j \in J} y_{ij} = 1, \forall i \in I \\ & y_{ij} \leq x_i, \forall i \in I, j \in J \\ & \sum_{i \in I} \sum_{k \in K} \theta_k d_{ik} y_{ij} + \psi \sum_{i \in I} \sum_{k \in K} \theta_k \hat{d}_{ik} y_{ij} \leq c_j, \forall j \in J \\ & p(t_{ij}) = \begin{cases} 0, & 0 \leq t_{ij} < ET \\ c_p(t_{ij} - ET), & ET \leq t_{ij} < LT, \forall i \in I, j \in J \\ +\infty, & t_{ij} \geq LT \end{cases} \\ & x_i \in \{0, 1\}, \forall i \in I \\ & y_{ij} \in \{0, 1\}, \forall i \in I, j \in J \end{aligned}$$

Proof of Proposition 2. Suppose $\sum_{i \in I} f_i x_i + \sum_{i \in I} \sum_{j \in J} p(t_{ij}) x_i = Q$. According to the definition of the box set, the uncertain patients' number can be written as:

$$\sum_{i \in I} \sum_{j \in J} \sum_{k \in K} c_t h_{ij} \theta_k d_{ik} y_{ij} + \sum_{i \in I} \sum_{j \in J} \sum_{k \in K} \zeta c_t h_{ij} \theta_k \hat{d}_{ik} y_{ij} + Q \leq H, (\zeta \in R^M : \|\zeta\|_\infty \leq \psi)$$

Then, we can obtain:

$$\sum_{i \in I} \sum_{j \in J} \sum_{k \in K} \zeta c_t h_{ij} \theta_k \hat{d}_{ik} y_{ij} \leq H - \sum_{i \in I} \sum_{j \in J} \sum_{k \in K} c_t h_{ij} \theta_k d_{ik} y_{ij} - Q, (\zeta \in R^M : \|\zeta\|_\infty \leq \psi)$$

In the worst case, we have:

$$\max_{\|\zeta\|_\infty \leq \psi} \sum_{i \in I} \sum_{j \in J} \sum_{k \in K} \zeta c_t h_{ij} \theta_k \hat{d}_{ik} y_{ij} \leq H - \sum_{i \in I} \sum_{j \in J} \sum_{k \in K} c_t h_{ij} \theta_k d_{ik} y_{ij} - Q$$

Because the maximum value on the left side of the inequality is $\psi \sum_{i \in I} \sum_{j \in J} \sum_{k \in K} c_t h_{ij} \theta_k \hat{d}_{ik} y_{ij}$,

the explicit constraint form can be obtained:

$$\sum_{i \in I} \sum_{j \in J} \sum_{k \in K} c_t h_{ij} \theta_k d_{ik} y_{ij} + \psi \sum_{i \in I} \sum_{j \in J} \sum_{k \in K} c_t h_{ij} \theta_k \hat{d}_{ik} y_{ij} + Q \leq H$$

Similarly, the robust counterpart of constraint 12 can be obtained. Therefore, the model based on the box uncertainty set is proved. \square

3.3.3. Ellipsoid Uncertainty Set

Proposition 3. *If the uncertain patients' number is defined as an ellipsoid set, that is, $Z_{ellipsoid} = \{\zeta \in R^M : \|\zeta\|_2 \leq \Omega\}$, Ω is the level of parameter uncertainty and the robust counterpart model in Section 3.3 can be built as follows:*

$$\begin{aligned} \min & \sum_{i \in I} f_i x_i + \sum_{i \in I} \sum_{j \in J} \sum_{k \in K} c_t h_{ij} \theta_k d_{ik} y_{ij} + \Omega \sqrt{\left(\sum_{i \in I} \sum_{j \in J} \sum_{k \in K} c_t h_{ij} \theta_k \hat{d}_{ik} y_{ij} \right)^2} + \sum_{i \in I} \sum_{j \in J} p(t_{ij}) x_i \\ \text{s.t.} & \sum_{i \in I} x_i \leq S \end{aligned}$$

$$\begin{aligned}
& \sum_{j \in J} y_{ij} = 1, \forall i \in I \\
& y_{ij} \leq x_i, \forall i \in I, j \in J \\
& \sum_{i \in I} \sum_{k \in K} \theta_k d_{ik} y_{ij} + \Omega \sqrt{\left(\sum_{i \in I} \sum_{k \in K} \theta_k \hat{d}_{ik} y_{ij} \right)^2} \leq c_j, \forall j \in J \\
& p(t_{ij}) = \begin{cases} 0, & 0 \leq t_{ij} < ET \\ c_p(t_{ij} - ET), & ET \leq t_{ij} < LT, \forall i \in I, j \in J \\ +\infty, & t_{ij} \geq LT \end{cases} \\
& x_i \in \{0, 1\}, \forall i \in I \\
& y_{ij} \in \{0, 1\}, \forall i \in I, j \in J
\end{aligned}$$

Proof of Proposition 3. Suppose $\sum_{i \in I} f_i x_i + \sum_{i \in I} \sum_{j \in J} p(t_{ij}) x_i = Q$. According to the definition of the ellipsoid set, the uncertain patients' number can be written as:

$$\sum_{i \in I} \sum_{j \in J} \sum_{k \in K} c_t h_{ij} \theta_k d_{ik} y_{ij} + \sum_{i \in I} \sum_{j \in J} \sum_{k \in K} \zeta c_t h_{ij} \theta_k \hat{d}_{ik} y_{ij} + Q \leq H, (\zeta \in R^M : \|\zeta\|_2 \leq \Omega)$$

Then, we can obtain:

$$\sum_{i \in I} \sum_{j \in J} \sum_{k \in K} \zeta c_t h_{ij} \theta_k \hat{d}_{ik} y_{ij} \leq H - \sum_{i \in I} \sum_{j \in J} \sum_{k \in K} c_t h_{ij} \theta_k d_{ik} y_{ij} - Q, (\zeta \in R^M : \|\zeta\|_2 \leq \Omega)$$

At worst case, we have:

$$\max_{\|\zeta\|_2 \leq \Omega} \sum_{i \in I} \sum_{j \in J} \sum_{k \in K} \zeta c_t h_{ij} \theta_k \hat{d}_{ik} y_{ij} \leq H - \sum_{i \in I} \sum_{j \in J} \sum_{k \in K} c_t h_{ij} \theta_k d_{ik} y_{ij} - Q$$

Consequently, the explicit form of the above formula can be obtained as:

$$\sum_{i \in I} \sum_{j \in J} \sum_{k \in K} c_t h_{ij} \theta_k d_{ik} y_{ij} + \Omega \sqrt{\left(\sum_{i \in I} \sum_{j \in J} \sum_{k \in K} c_t h_{ij} \theta_k \hat{d}_{ik} y_{ij} \right)^2} + Q \leq H$$

Similarly, the robust counterpart of constraint 12 can be obtained. Therefore, the model based on the ellipsoid uncertainty set is proved. \square

4. Simulations

In order to verify the proposed method, this section shows an emergency management example under COVID-19.

4.1. Background and Data Sources

This paper chooses Huanggang City to conduct a numerical experiment, which was severely affected by the coronavirus. Huanggang has a total of 10 administrative areas. We took the township as the emergency demand points unit to carry out the detailed division for a total of 127 demand points. The emergency medical facility point is a large open area with flat terrain and convenient transportation. A total of 30 points are selected. Simultaneously, seven large rear hospitals with grades II and above were selected. The number of people per emergency demand point was obtained from the National Bureau of Statistics in 2017, while the number of confirmed COVID-19 patients in Huanggang was obtained from the National Health Commission of the People's Republic of China released on 21 March 2020.

The selection of emergency facilities is based on the service capacity (i.e., Hongshan stadium), that is, $c_e = \frac{\text{venues beds}}{\text{venues area}} \times \text{facilities point area}$. The attraction factor of the facility point is calculated by the hospitals' number within 10 km of each facility point. The reference attraction factor was one, and the attraction factor increased by 0.1 for each additional hospital, and so on. The relevant data of the demand points, emergency medical facility points, large rear hospitals, and the number of patients are shown in Tables 2–5, respectively. The detailed distribution of the residents' demand points, candidate facility points, and large rear hospitals is shown in Figure 2. The color distribution of each administrative area is determined according to the number of local patients with COVID-19. The more patients, the darker the color will be.

Table 2. Latitude and longitude coordinates of demand points and population size.

No.	Coordinate	Population	No.	Coordinate	Population	No.	Coordinate	Population
1	114.66064,31.45983	80,798	44	115.65594,30.76541	19,731	87	115.69542,30.30748	50,072
2	114.60284,31.27431	119,425	45	115.63523,30.88881	22,065	88	115.85314,30.51451	30,936
3	114.49922,31.28993	39,658	46	115.75470,30.99033	32,412	89	115.82113,30.31645	36,759
4	114.55444,31.15556	50,883	47	115.90135,31.00211	18,108	90	115.56911,29.85114	161,582
5	114.56646,31.05605	32,145	48	115.75740,30.88672	32,279	91	115.56400,29.85043	34,026
6	114.44895,31.30736	35,447	49	115.76842,30.81582	42,325	92	115.42095,29.91312	18,948
7	114.64585,31.02003	30,639	50	115.61337,30.64183	25,045	93	115.70016,29.88795	4083
8	114.64488,30.96300	23,432	51	115.63833,30.83598	19,318	94	115.61056,30.11381	113,247
9	114.70241,31.14612	56,044	52	115.93407,30.90572	7477	95	115.73690,30.08317	50,297
10	114.53016,31.45716	43,804	53	114.86957,30.63203	71,185	96	115.71488,30.01275	64,690
11	114.64299,31.28841	86,479	54	114.88533,30.74325	57,183	97	115.62547,29.93993	44,857
12	114.66770,31.38754	2049	55	115.07828,30.69643	24,063	98	115.61438,29.99534	35,921
13	114.99998,31.16661	55,601	56	115.19036,30.76037	41,226	99	115.55408,30.02849	32,203
14	115.02587,31.18524	68,485	57	115.09952,30.64720	29,827	100	115.47552,29.94930	47,311
15	115.04128,31.17716	80,722	58	115.02658,30.65196	19,640	101	115.70678,29.86632	37,082
16	114.80704,31.06828	50,109	59	114.98275,30.60512	32,134	102	115.93927,30.07392	141,488
17	115.12917,31.20715	31,297	60	115.08718,30.79427	19,117	103	115.92131,29.88258	98,543
18	115.01422,31.03803	61,839	61	115.05516,30.79163	18,816	104	115.98622,29.75636	97,956
19	114.88605,31.12271	42,918	62	114.93149,30.67896	22,811	105	116.00873,30.05003	21,945
20	114.98878,31.35650	47,632	63	115.26651,30.43888	193,988	106	115.84793,30.08979	59,759
21	115.09380,31.47408	36,169	64	115.02802,30.42591	113,356	107	115.98671,30.21229	33,323
22	115.18852,31.07276	36,567	65	115.34092,30.55166	71,852	108	115.94173,30.17009	13,971
23	115.17771,30.96000	32,079	66	115.12536,30.59354	66,860	109	115.89000,30.00755	65,122
24	115.31886,31.04682	37,066	67	115.17918,30.61747	49,785	110	115.80776,29.87894	71,168
25	115.23286,31.32758	40,083	68	115.23300,30.72709	78,925	111	115.82248,29.81693	55,883
26	115.07628,31.37152	34,513	69	115.44597,30.59109	14,885	112	116.03935,30.07820	27,127
27	114.83977,31.33245	43,233	70	115.41237,30.56442	35,562	113	115.90764,29.78591	47,872
28	114.75598,31.01214	20,520	71	115.47997,30.46645	49,312	114	115.95513,30.27099	12,357
29	115.03054,30.96647	26,470	72	115.27209,30.38250	35,922	115	115.98193,30.10304	34,299
30	115.37487,31.18694	37,992	73	115.11897,30.23280	60,655	116	115.90153,30.13119	27,634
31	114.84998,31.03664	40,457	74	115.14533,30.35013	48,792	117	116.10982,29.83206	15,919
32	115.27363,30.83227	57,980	75	115.53676,30.52150	22,214	118	114.88374,30.44167	156,011
33	115.46262,31.12651	59,219	76	115.44136,30.25094	150,600	119	114.90441,30.47002	21,939
34	115.67112,31.14024	30,041	77	115.33968,30.07489	67,040	120	114.88198,30.47291	22,977
35	115.60163,31.00290	29,204	78	115.38161,30.30637	68,543	121	114.97287,30.45216	16,593
36	115.47994,30.84096	30,825	79	115.50228,30.36850	30,920	122	114.94966,30.48861	21,550
37	115.19510,30.81844	35,918	80	115.61687,30.38513	42,447	123	114.91279,30.54566	25,416
38	115.39093,30.98976	50,823	81	115.79129,30.41924	42,065	124	115.03657,30.59585	25,856
39	115.55835,30.69722	59,270	82	115.80244,30.49354	19,624	125	114.98103,30.53740	19,654
40	115.40694,30.68214	33,132	83	115.42998,30.20307	49,666	126	115.00178,30.58077	4753
41	115.39610,30.78371	114,890	84	115.28774,30.14920	20,547	127	114.91652,30.44885	52,020
42	115.67654,30.74001	121,669	85	115.28122,30.27222	35,569			
43	115.61889,30.59068	16,027	86	115.58902,30.29642	67,756			

Table 3. Coordinates, service capacity, and attraction factors of candidate facility points.

No.	Coordinate	Capacity	Attraction Factor	No.	Coordinate	Capacity	Attraction Factor
1	114.63284,31.31431	27,840	1.3	16	114.89070,30.64937	4478	1.3
2	115.00939,31.16563	17,043	1.2	17	115.70328,30.81313	90,032	1.1
3	114.73256,31.10384	9100	1.1	18	114.95961,30.52801	29,708	1.2
4	115.95857,30.09049	118,450	1	19	115.41705,30.79636	49,879	1.3
5	115.55704,30.00018	6998	1.2	20	115.78056,30.90014	5282	1.2
6	115.10718,31.31427	10,989	1.4	21	115.38103,30.49740	73,502	1
7	114.62315,31.29476	104,917	1.1	22	115.20200,30.48535	8220	1.1
8	114.93146,30.62063	73,426	1.2	23	115.62718,30.00019	64,520	1.1
9	115.08277,30.23464	30,964	1.3	24	114.98103,30.53740	7598	1.2
10	115.02813,31.18019	35,097	1.1	25	115.05760,30.52585	45,008	1.4
11	115.93927,30.11392	9320	1	26	115.02813,31.18019	2890	1
12	115.01814,31.17779	3233	1.2	27	115.09380,30.96408	5354	1.1
13	114.90714,30.43954	52,560	1.1	28	115.41122,30.23686	6210	1.2
14	115.16036,30.64037	39,088	1	29	114.89070,30.64937	10,879	1.2
15	115.43629,30.23262	8352	1.4	30	115.55681,29.85051	4877	1.1

Table 4. Coordinates and number of beds in the large rear hospitals.

No.	Coordinate	Number of Beds	No.	Coordinate	Number of Beds
1	114.62522,31.28687	810	5	114.89880,30.47378	600
2	115.03035,31.18547	560	6	115.59644,29.87249	400
3	115.66802,30.73284	780	7	115.95089,30.08262	350
4	114.88141,30.45194	1050			

Table 5. The number of cases in each region.

Region	Number of Patients	Region	Number of Patients
Huangzhou District	968	Xishui County	303
Tuanfeng County	173	Qichun County	265
Hongan County	316	Huangmei County	284
Luotian County	69	Macheng County	243
Yingshan County	62	Wuxue County	224

The distance between the two points was calculated according to the longitude and latitude coordinates. Equation (33) can be utilized to convert the coordinates of longitude and latitude into the actual traveling distance h_{ij} between the two nodes i and j .

$$h_{ij} = k \cdot \frac{\sqrt{(x_i - x_j)^2 + (y_i - y_j)^2}}{180} \cdot \pi \cdot 6370 \quad (33)$$

Here, $(x_i, y_i), (x_j, y_j)$ is the longitude and latitude coordinates of the two points. The radius of the earth is 6370 (km). The formula $\frac{\sqrt{(x_i - x_j)^2 + (y_i - y_j)^2}}{180} \cdot \pi \cdot 6370$ is used to calculate the linear distance between the two points. The linear distance of the two points for 50 groups was extracted, and we compared this with the actual driving distance obtained from the Baidu map. The error value was obtained.

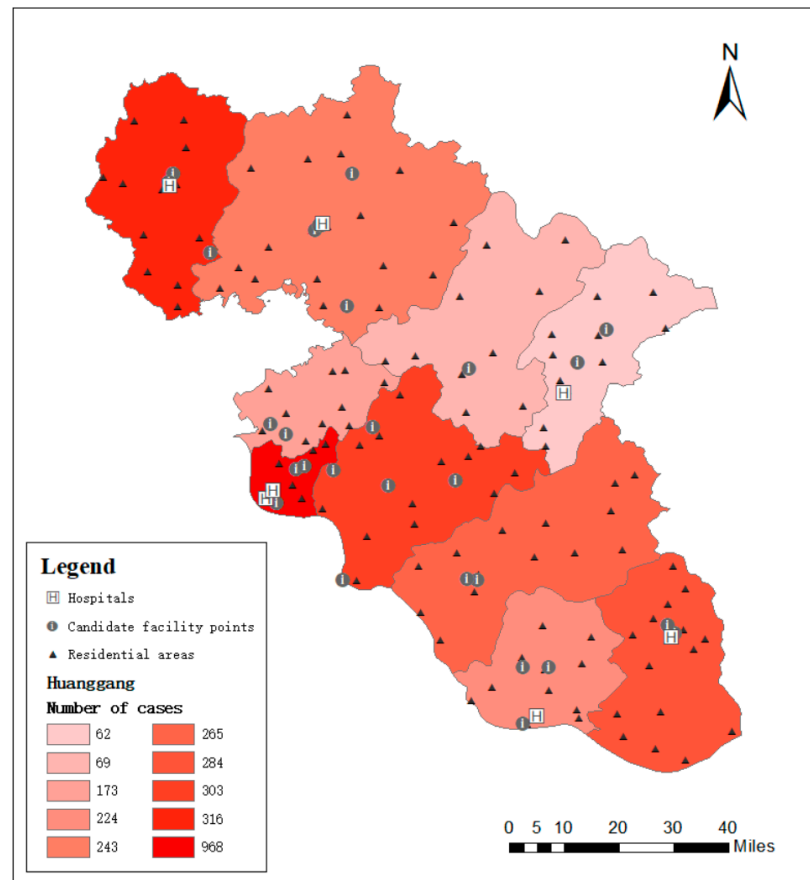


Figure 2. Distribution of demand points, candidate facility points, and base hospitals.

4.2. The Alternative Facilities Selection Based on EWM

The initial index data matrix of the candidate emergency medical facility points is composed of the following factors: the construction cost of facilities, transportation convenience, the patients’ number that can be accommodated, regional population density, the accessibility of patients, and the number of hospitals within 10 km. Among them, the construction cost of the facility point is calculated at 1000 yuan per square meter. Transportation convenience is determined by the distance between the facility point and the nearest provincial or national highway. The accessibility of patients is determined based on the maximum time it takes for the demand point to reach the candidate facility point. The regional population density (10,000 people per square kilometer) is obtained according to the area and population of the region.

According to Equations (5) and (6), the information entropy value and weight vector of the six evaluation indexes for the normalized matrix are obtained, as shown in Table 6. Meanwhile, the comprehensive evaluation score of each candidate emergency medical facility is calculated, $s_i = (0.3395; 0.3860; 0.1694; 0.8913; 0.1325; 0.4670; 0.7570; 0.6649; 0.4847; 0.6181; 0.2177; 0.2641; 0.6105; 0.6263; 0.2178; 0.1831; 0.6789; 0.4127; 0.5967; 0.1523; 0.6507; 0.0876; 0.6078; 0.1077; 0.3519; 0.1659; 0.1309; 0.2888; 0.2024; 0.1601)$.

Table 6. Information entropy and entropy weight.

	1	2	3	4	5	6
Information entropy ε_j	0.86431	0.96559	0.83973	0.95249	0.91932	0.94877
Entropy weight w_j	0.26617	0.06749	0.31439	0.09319	0.15826	0.10049

According to the comprehensive evaluation value S_i , ten emergency medical facilities with high evaluation values were selected: 4, 7, 8, 10, 13, 14, 17, 19, 21, and 23.

4.3. Robust Solution Process

After the alternative emergency medical facilities are selected by EWM, large rear hospitals should be configured rationally to ensure that severe patients can receive timely treatment. According to Equation (33), the distance h_{ij} between each facility point and the base hospital is obtained, as shown in Table 7. Other relevant parameters are set as: $c_t = 10$, $c_p = 6$, $\bar{v}_j = 35$ km/h, $ET = 120$ min, $LT = 480$ min, $\theta_1 = 1$, $\theta_2 = 0.5$, $\theta_3 = 0.1$. When the uncertain level Γ_k is considered, it is assumed that the variation amplitude of the corresponding constraints is equal (i.e., $\Gamma_k = \Gamma$) and Γ is an all integer. In this paper, MATLAB R2016a was utilized for programming, and CPLEX was called to solve the problem under the experimental environment of 8 GB memory and 1.60 GHz CPU with Intel Core i5.

Table 7. The distance between each facility points and the large rear hospital.

Facility Points	Large Base Rear Hospital						
	J_1	J_2	J_3	J_4	J_5	J_6	J_7
I_4	199.1641	319.1826	235.1414	505.2721	626.4589	281.9618	8.558354
I_7	0.906985	93.74792	395.6967	392.0141	481.4094	1149.629	1399.142
I_8	81.52122	127.5054	248.5002	78.25099	46.62485	667.7027	897.0696
I_{10}	46.33759	1.272584	260.4087	330.3708	399.213	951.1418	1115.944
I_{13}	99.2809	168.108	271.98	12.69828	19.58887	595.4059	858.4737
I_{14}	93.30548	124.6055	172.1071	149.7007	72.38121	589.0629	752.9345
I_{17}	130.9173	171.0052	29.24747	399.2292	485.3551	631.5039	600.2825
I_{19}	103.5559	121.9797	86.34575	283.1968	339.3343	627.7912	693.6411
I_{21}	121.5096	171.719	63.80801	223.1036	268.3869	440.9306	548.5269
I_{23}	181.3071	295.079	244.7432	387.752	482.9592	87.61668	259.9675

4.4. Result Analysis

When the disturbance ratio is 2%, and the uncertain level is $\Gamma = 5$, the configuration scheme is (4-7,7-1,8-5,10-2,13-4,14-5,17-3,19-3,21-5,23-6). The specific configuration scenario is shown in Figure 3. The green dot is the demand point of the residents, the blue square is the selected emergency medical facility point, and the red five-pointed star is the large rear hospital. The connecting line indicates the service relationship between the demand point, the facility point, and the base hospital. As can be seen from Figure 3, the needs of residents in each township have been met. The alternative emergency medical facility points (4,7,8,10,13,14,17,19,21,23) have corresponding large base hospitals to provide first-aid support to ensure the further transfer and treatment of critically ill patients. In addition, the optimal facility points are evenly distributed. One emergency medical facility has been established in each of the 10 administrative regions of Huanggang to ensure that the needs of the residents in each administrative region can be effectively covered by the emergency medical facility points. Additionally, the total traveled distance can be reduced. Similarly, we can obtain configuration plans in other scenarios. Due to space limitations, these will not be displayed here.

The change in the optimal configuration scheme with a different uncertain level Γ and disturbance proportions is shown in Table 8. The optimal configuration scheme between the large base hospital and emergency medical facilities has also changed with the presence of uncertain patient numbers.

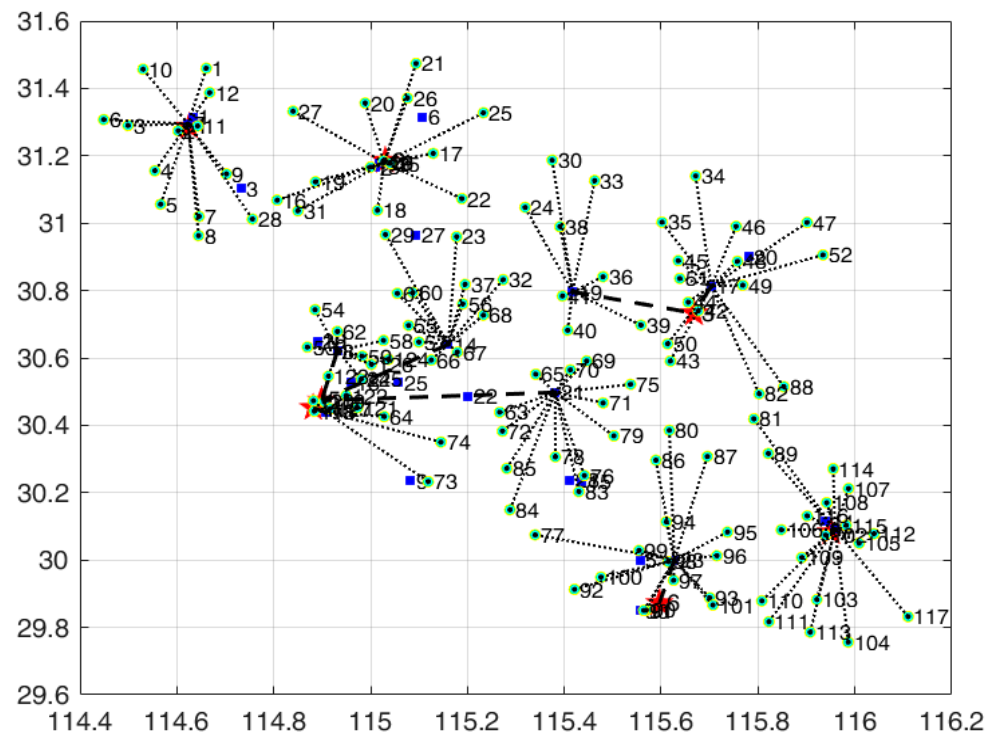


Figure 3. Configuration scenario with 2% disturbance ratio and $\Gamma = 5$.

Table 8. Configuration scheme with different disturbance proportions and uncertainty levels.

Γ	Disturbance in Proportion			
	2%	5%	10%	20%
0	4-7,7-1,8-5,10-2,13-4,14-5,17-3,19-3,21-3,23-6	4-7,7-1,8-5,10-2,13-4,14-5,17-3,19-3,21-3,23-6	4-7,7-1,8-5,10-2,13-4,14-5,17-3,19-3,21-3,23-6	4-7,7-1,8-5,10-2,13-4,14-5,17-3,19-3,21-3,23-6
2	4-7,7-1,8-5,10-2,13-4,14-5,17-3,19-3,21-5,23-6	4-7,7-1,8-5,10-2,13-4,14-5,17-3,19-3,21-5,23-6	4-7,7-1,8-4,10-2,13-5,14-5,17-3,19-3,21-5,23-6	4-7,7-1,8-4,10-2,13-5,14-5,17-3,19-3,21-5,23-6
4	4-7,7-1,8-5,10-2,13-4,14-5,17-3,19-3,21-5,23-6	4-7,7-1,8-5,10-2,13-4,14-5,17-3,19-3,21-5,23-6	4-7,7-1,8-4,10-2,13-5,14-5,17-3,19-3,21-5,23-6	4,17-3,19-2,21-5,23-6
6	4-7,7-1,8-4,10-2,13-5,14-5,17-3,19-3,21-5,23-6	4-7,7-1,8-4,10-2,13-5,14-5,17-3,19-3,21-5,23-6	4-7,7-1,8-4,10-2,13-5,14-4,17-3,19-2,21-5,23-6	4-7,7-1,8-4,10-2,13-5,14-4,17-3,19-2,21-5,23-6
8	4-7,7-1,8-4,10-2,13-5,14-4,17-3,19-2,21-5,23-6	4-7,7-1,8-4,10-2,13-5,14-4,17-3,19-2,21-5,23-6	4-7,7-1,8-4,10-2,13-5,14-4,17-3,19-2,21-5,23-7	4-7,7-1,8-4,10-2,13-5,14-4,17-3,19-2,21-5,23-7
10	4-7,7-1,8-4,10-2,13-5,14-4,17-3,19-2,21-5,23-6	4-7,7-1,8-4,10-2,13-5,14-4,17-3,19-2,21-5,23-7	4-7,7-1,8-4,10-2,13-5,14-4,17-3,19-2,21-5,23-7	4-7,7-1,8-4,10-2,13-5,14-4,17-3,19-2,21-5,23-7

The change in the total cost with a different uncertainty level Γ and disturbance proportions is shown in Figure 4. When $\Gamma = 0$, the robust model is equivalent to the deterministic model, and the total cost is 4.47009×10^9 . Compared with the robust configuration model, the emergency medical facilities configuration deterministic model (EMFC) is not robust because it does not take into account the uncertain number of patients at the emergency medical points, so it has a certain deviation from the actual situation. As can be seen from Figure 4, the total cost increases with the increase in the uncertainty level Γ when the disturbance proportion remains unchanged. Additionally, the higher the disturbance proportion is, the higher the total cost will be when the uncertainty level remains unchanged. Simultaneously, the uncertainty level Γ can measure the risk preference of decision-makers to some extent. Accordingly, decision-makers can choose the optimal combination of uncertainty levels and the disturbance proportion according to their preference degree to the uncertain risk. If the decision-maker pursues a preference for risk, he can choose a small level of

uncertainty and disturbance ratio. However, he must bear the possible losses caused by uncertainty in mind. If the decision-maker has a preference for risk aversion, he can select a large uncertainty level and disturbance proportion to provide a large probability guarantee for the effectiveness and feasibility of the configuration scheme. However, the total cost of the system operation will increase. If the decision-maker is risk neutral, he can choose a compromise.

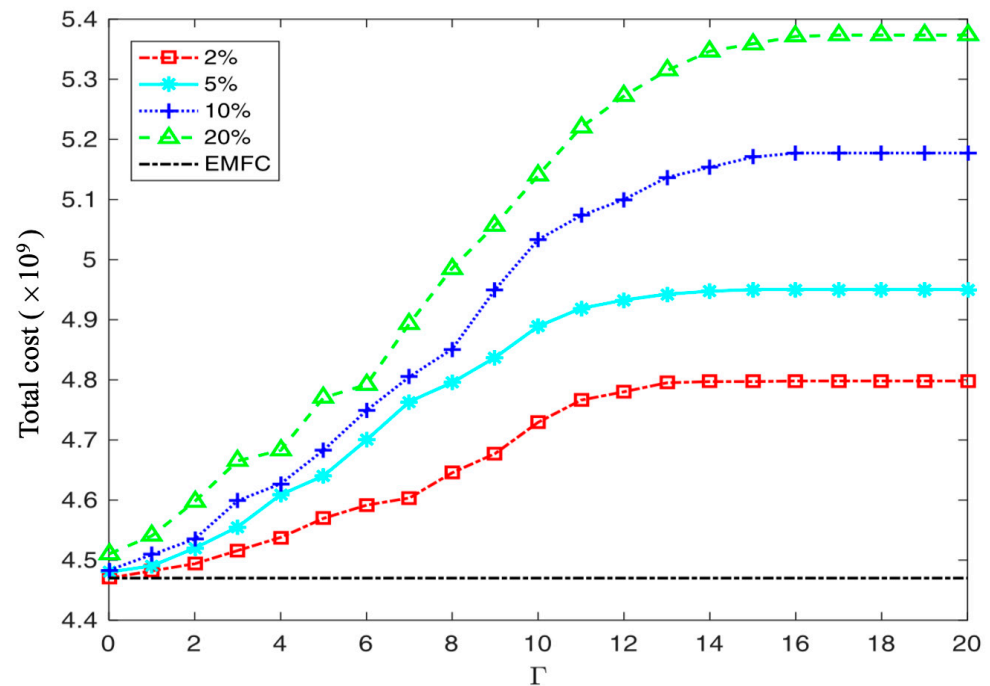


Figure 4. The total cost varies with different disturbance proportions and Γ .

It is worth mentioning that although the total cost varies with different disturbance proportions and uncertainty levels, there are only six configuration schemes. This further indicates that the model has good robustness, and the optimal scheme is not sensitive to parameter perturbation. Among them, the solution of the deterministic model is (4-7,7-1,8-5,10-2,13-4,14-5,17-3,19-3,21-3,23-6), as shown in Figure 5. The former number represents the emergency medical facility point, and the latter number indicates the large rear hospital that serves it when a patient is in an emergency. The blue dot in the figure represents the whole emergency medical facility, the red five-pointed star represents the large rear base hospital, and the black dotted line shows the service relationship between the emergency medical facility and the base hospital. When the disturbance proportion and uncertainty level Γ are small, the configuration scheme is (4-7,7-1,8-5,10-2,13-4,14-5,17-3,19-3,21-5,23-6), as shown in Figure 6. Additionally, the decision-maker with a risk preference can choose this scheme. When the disturbance proportion and uncertainty level Γ are large, the configuration scheme is (4-7,7-1,8-4,10-2,13-5,14-4,17-3,19-2,21-5,23-7), as shown in Figure 7. Additionally, the decision-maker with a risk aversion can choose this scheme. The rest of the configuration schemes are (4-7,7-1,8-5,10-2,13-5,14-5,17-3,19-3,21-5,23-6), (4-7,7-1,8-4,10-2,13-5,14-5,17-3,19-3,21-5,23-6), and (4-7,7-1,8-4,10-2,13-5,14-4,17-3,19-2,21-5,23-6). In this case, the decision-maker with risk neutrality can choose this solution. We will not show the configuration scheme figures here.

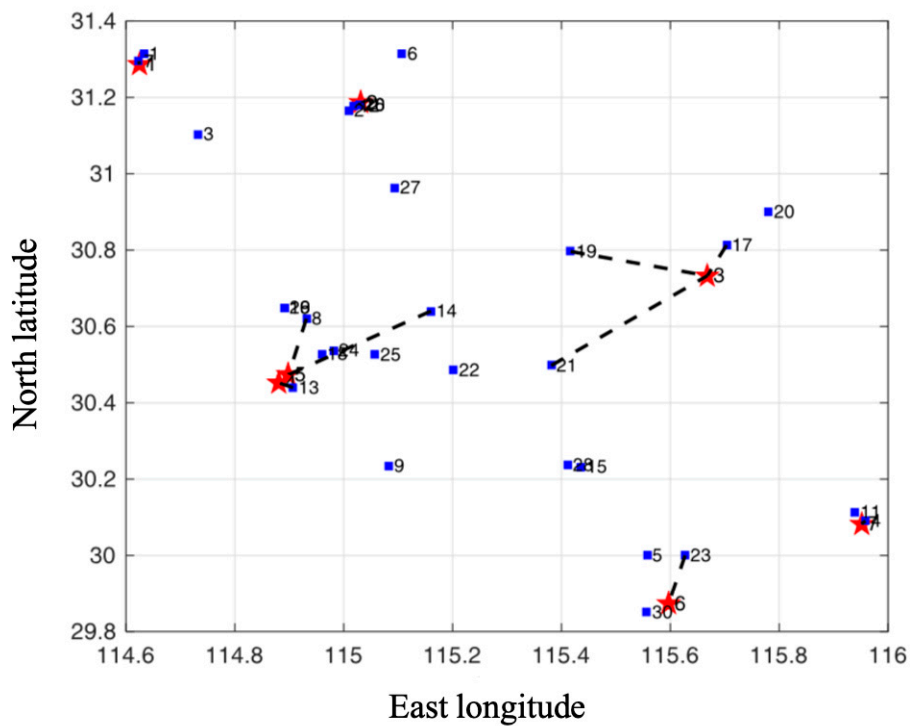


Figure 5. The configuration scheme with $\Gamma = 0$.

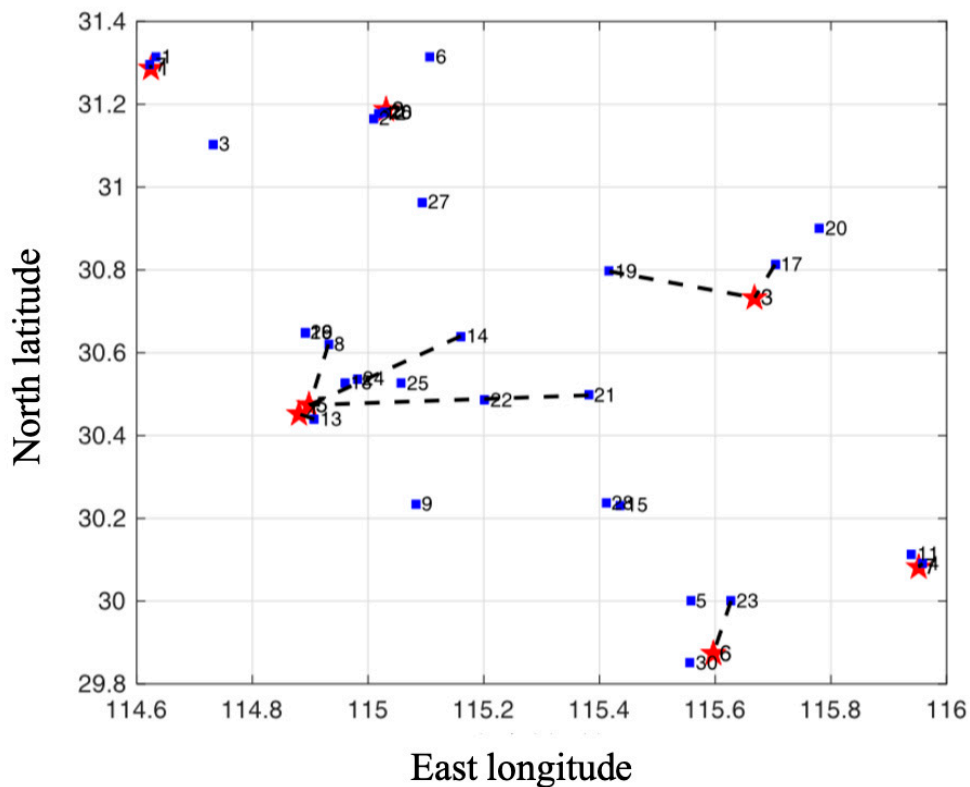


Figure 6. The configuration scheme with $\Gamma = 2$.

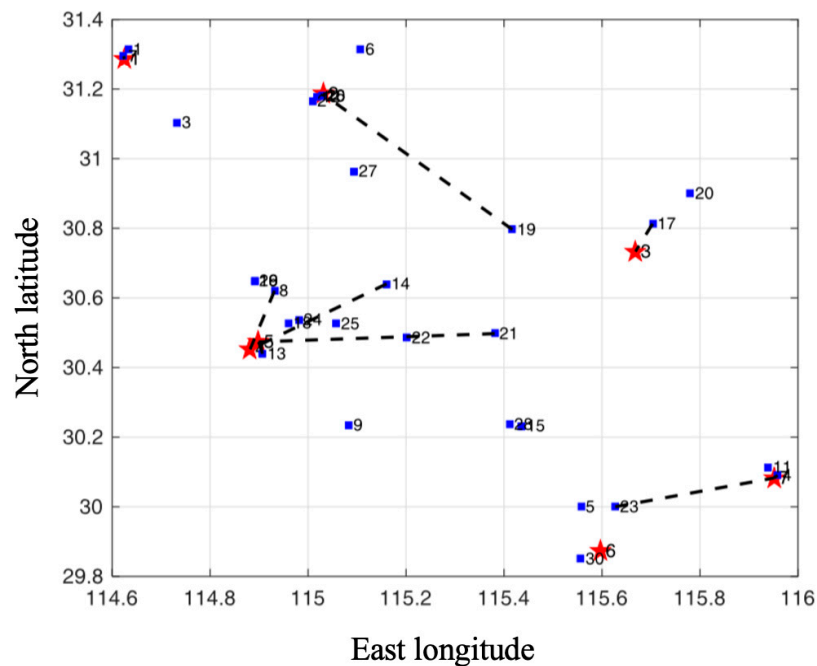


Figure 7. The configuration scheme with $\Gamma = 10$.

The calculation time of each scheme is shown in Figure 8. The shortest time is 1.9127 s, and the longest time is 11.6776 s. Additionally, the average time is 7.54 s, which meets the actual demand. As can be seen from Figure 8, compared with the robust configuration model, the deterministic EMFC model is not robust because it does not take into account the uncertain number of patients at the emergency medical points. Therefore, the solution time of the EMFC model is not sensitive to uncertain level parameters Γ . When the Γ is small, the solution time is relatively short. When the Γ is large, the solution time increases. This is because the increase in the uncertainty level leads to an increase in the search range of the solution, which in turn leads to an increase in the solution time. However, the longest solution time is only about 12 s, which fully meets the actual demand.

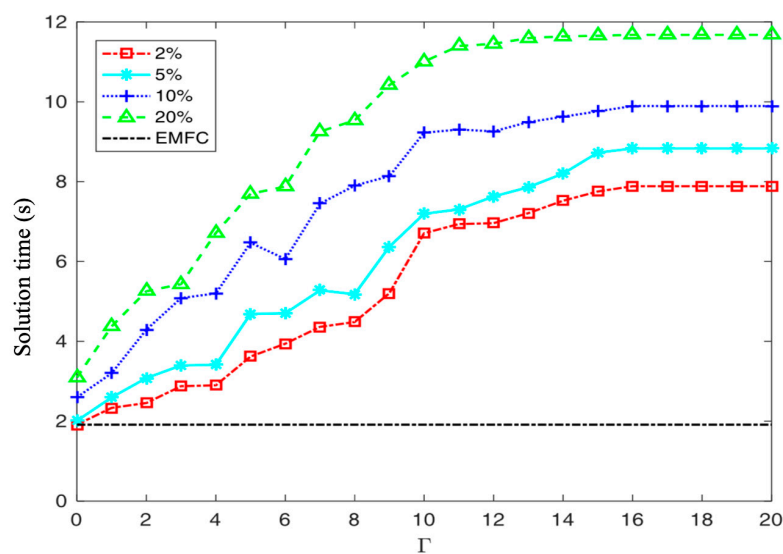


Figure 8. The total solution time varies with different disturbance proportions and Γ .

To sum up, this paper takes Huanggang City as an example to provide the optimal emergency medical facilities location and configuration scheme under COVID-19. Moreover, the impact of uncertain parameters on the total target cost, configuration scheme, and

solution time of the model is deeply analyzed. Additionally, the feasibility and robustness of the proposed method are verified.

5. Conclusions

5.1. Discussions

This paper investigates a hierarchical diagnosis and treatment system for emergency medical facilities' location-allocation under uncertain circumstances. Firstly, taking into account the ease of the centralized utilization of medical resources, we adopted EWM to select alternative facilities from the whole of the facilities. Secondly, three uncertainty sets were introduced to describe the uncertainty of the patients' number. A robust optimization model with capacity and time window constraints was constructed to configure the large rear hospital to ensure the timely treatment of patients. The comparison between Figures 4 and 8 shows that although the total cost and solution time of the deterministic location-allocation model is lower, the deterministic model is not robust and cannot effectively describe the uncertain number of patients under the epidemic situation. However, the robust optimization model proposed in this paper not only considers the actual uncertain number of patients but also does not need to know the probability distribution of the number of patients in advance. Additionally, the solution time of the robust model is less than 12 s, which is very consistent with the actual situation. Finally, numerical simulation experiments were conducted to solve the emergency medical facilities' location and configuration in Huanggang City under COVID-19. The results show that the location-allocation decision method proposed in this paper is scientific and effective. The proposed method can meet the treatment needs of patients after public health emergencies and effectively reduce driving time.

During the epidemic period, the hierarchical diagnosis and treatment mode avoids the paralysis of large hospitals caused by the concentration of a large number of patients. It significantly improves the use efficiency of medical resources. This study proposes a hybrid approach of emergency medical facility location-allocation. We have a two-step plan for post-outbreak isolation and treatment. In the first stage, 10 facilities with the highest scores are selected from 30 facilities by EWM, which are regarded as community emergency medical points. When there are critical patients who cannot be handled by community medical centers, the second stage is to send the critical patients to large base hospitals for treatment.

The hierarchical diagnosis and treatment mode plays an obvious role in reversing the unreasonable pattern of medical resource allocation and solving the problem of unbalanced medical resource allocation during the epidemic period. Based on the construction of a coordinated medical and health service network between urban and rural areas, the hierarchical diagnosis and treatment mode has rationally allocated medical resources, effectively revitalized the stock of medical resources, and improved the allocation and use efficiency of medical resources by relying on the majority of hospitals and grassroots medical and health institutions. The most economical and effective measures to deal with the epidemic are to improve the level of community medical care and complete the system. Therefore, this study has a certain practical significance for public health authorities to improve the scientific level of epidemic prevention and control.

5.2. Future Directions

The proposed method in this paper can provide a scientific and reasonable reference for decision-makers to choose the optimal facility layout plan. In order to further improve the practical application value of the proposed model, future research work will refine the factors affecting the location decision. Additionally, we could consider the existence of various factors, such as the traffic time uncertainty under different road congestion conditions and resource constraints, and isolation from the public, so as to further investigate the robust optimization model. In future research directions, we can also consider the impact of facility interruption on the hierarchical diagnosis system, which will make the emergency

medical location-allocation model more realistic. Meanwhile, this paper only studies the budgeted uncertainty model. The next work can be compared with the box uncertainty model and ellipsoid uncertainty model, which can further illustrate the effectiveness of the proposed method.

In addition, group consensus plays an important role in decision-making [55–58]. In future studies, we can invite experts from different fields to help emergency management departments make better decisions through the consensus-building process. There are various methods for facility location. This paper only studies the impact of the robust optimization method on facility location. In the future, we can extend the fuzzy rough decision-making approach [59] and multi-criteria decision-making [60] to the emergency medical facilities location. Supply chains have become a hot research field in recent years [61]. In the future, we can study how to improve the fairness and efficiency of supply chains in the transportation of emergency medical supplies. In the future, we can consider adding machine learning [62] methods to the location of emergency medical facilities.

Author Contributions: Conceptualization, L.W. and M.Y.; data curation, F.X. and M.Y.; formal analysis, L.W. and M.Y.; investigation, F.X. and S.Q.; methodology, L.W. and M.Y.; resources, F.X.; validation, F.X. and M.Y.; writing—original draft, L.W. and M.Y.; writing—review and editing, F.X., S.Q. and M.Y. All authors have read and agreed to the published version of the manuscript.

Funding: This research was supported by the National Natural Science Foundation of China (No. 72171149, 72171123).

Institutional Review Board Statement: Not applicable.

Informed Consent Statement: Not applicable.

Data Availability Statement: The data used to support the findings of this study are available from the database with the web address <http://www.nhc.gov.cn/> (accessed on 21 March 2020). The data presented in this study are available on request from the corresponding author.

Acknowledgments: The authors would like to thank the anonymous reviewers for their comments and suggestions.

Conflicts of Interest: The authors declare that they have no conflicts of interest.

References

1. Liu, J.; Bai, J.Y.; Wu, D.S. Medical supplies scheduling in major public health emergencies. *Transp. Res. Part E Logist. Transp. Rev.* **2021**, *154*, 102464. [[CrossRef](#)]
2. Xu, Y.; Li, J.; Liu, Y.W. Quantitative evaluation of provincial government plans for public health emergencies in China. *Int. J. Disast. Risk Reduct.* **2022**, *81*, 103292. [[CrossRef](#)]
3. Alsafi, R.T. Lessons from SARS-CoV, MERS-CoV, and SARS-CoV-2 Infections: What We Know So Far. *Can. J. Infect. Dis. Med.* **2022**, *2022*, 1156273. [[CrossRef](#)] [[PubMed](#)]
4. Hartt, M. COVID-19: A lonely pandemic. *Cities Health* **2021**, *5*, S80–S82. [[CrossRef](#)]
5. Zhang, X.; Ding, Z.J.; Hang, J.Q.; He, Q.Z. How do stock price indices absorb the COVID-19 pandemic shocks? *N. Am. J. Econ. Financ.* **2022**, *60*, 101672. [[CrossRef](#)]
6. Zhu, L.; Chen, P.L.; Dong, D.D.; Wang, Z.X. Can artificial intelligence enable the government to respond more effectively to major public health emergencies? Taking the prevention and control of Covid-19 in China as an example. *Socio Econ. Plan. Sci.* **2022**, *80*, 101029. [[CrossRef](#)]
7. Liu, M.; Xu, X.F.; Cao, J.; Zhang, D. Integrated planning for public health emergencies: A modified model for controlling H1N1 pandemic. *J. Oper. Res. Soc.* **2020**, *71*, 748–761. [[CrossRef](#)]
8. Zhang, L.; Zhao, W.J.; Sun, B.B.; Huang, Y.; Glänzel, W. How scientific research reacts to international public health emergencies: A global analysis of response patterns. *Scientometrics* **2020**, *124*, 747–773. [[CrossRef](#)]
9. Jin, R.; Xia, T.; Liu, X.; Murata, T.; Kim, K.S. Predicting Emergency Medical Service Demand With Bipartite Graph Convolutional Networks. *IEEE Access* **2021**, *9*, 9903–9915. [[CrossRef](#)]
10. Xu, Z.Q.; Cheng, Y.K.; Yao, S.L. Tripartite Evolutionary Game Model for Public Health Emergencies. *Discrete Dyn. Nat. Soc.* **2021**, *2021*, 6693597. [[CrossRef](#)]
11. Tessema, F.S.; Koya, P.R.; Bole, B.K. Optimal Control and Cost-Effectiveness Analysis of Cholera with Vaccination. *J. Math.* **2022**, *2022*, 1705277. [[CrossRef](#)]

12. Deng, X.C. Location-Routing Problem of Emergency Facilities under Uncertain Demand by Branch-Price and Cut. *J. Math.* **2021**, *2021*, 9152989. [[CrossRef](#)]
13. Yang, N.; Shen, L.Y.; Shu, T.H.; Liao, S.J.; Peng, Y.; Wang, J.H. An integrative method for analyzing spatial accessibility in the hierarchical diagnosis and treatment system in China. *Soc. Sci. Med.* **2021**, *270*, 113656. [[CrossRef](#)] [[PubMed](#)]
14. Schullerus, G.; Supavatanakul, P.; Krebs, V.; Lunze, J. Modelling and hierarchical diagnosis of timed discrete-event systems. *Math. Comp. Model. Dyn.* **2006**, *12*, 519–542. [[CrossRef](#)]
15. Toregas, C.; Swain, R.; ReVelle, C.; Bergman, L. The Location of Emergency Service Facilities. *Oper. Res.* **1971**, *19*, 1363–1373. [[CrossRef](#)]
16. He, Q.Z.; Tong, H.; Liu, J.B. How Does Inequality Affect the Residents' Subjective Well-Being: Inequality of Opportunity and Inequality of Effort. *Front. Psychol.* **2022**, *13*, 843854. [[CrossRef](#)] [[PubMed](#)]
17. Gigovic, L.; Pamucar, D.; Bozanic, D.; Ljubojevic, S. Application of the GIS-DANP-MABAC multi-criteria model for selecting the location of wind farms: A case study of Vojvodina, Serbia. *Renew. Energ.* **2017**, *103*, 501–521. [[CrossRef](#)]
18. Biswas, S.; Pamucar, D. Facility Location Selection for B-Schools in Indian Context: A Multi-Criteria Group Decision Based Analysis. *Axioms* **2020**, *9*, 77. [[CrossRef](#)]
19. Pamucar, D.; Gigovic, L.; Bajic, Z.; Janosevic, M. Location Selection for Wind Farms Using GIS Multi-Criteria Hybrid Model: An Approach Based on Fuzzy and Rough Numbers. *Sustainability* **2017**, *9*, 1315. [[CrossRef](#)]
20. Boonmee, C.; Arimura, M.; Asada, T. Facility location optimization model for emergency humanitarian logistics. *Int. J. Disast. Risk Reduct.* **2017**, *24*, 485–498. [[CrossRef](#)]
21. Zhang, H.Z.; Zhang, K.; Chen, Y.T.; Ma, L. Multi-objective two-level medical facility location problem and tabu search algorithm. *Inf. Sci.* **2022**, *608*, 734–756. [[CrossRef](#)]
22. Liu, K.N. GIS-based MCDM framework combined with coupled multi-hazard assessment for site selection of post-earthquake emergency medical service facilities in Wenchuan, China. *Int. J. Disast. Risk Reduct.* **2022**, *73*, 102873. [[CrossRef](#)]
23. Yücel, E.; Salman, F.S.; Bozkaya, B.; Gökalp, C. A data-driven optimization framework for routing mobile medical facilities. *Ann. Oper. Res.* **2020**, *291*, 1077–1102. [[CrossRef](#)]
24. Zhen, L.; Wang, K.; Liu, H.C. Disaster Relief Facility Network Design in Metropolises. *IEEE Trans. Syst. Man Cybern. Syst.* **2015**, *45*, 751–761. [[CrossRef](#)]
25. Ji, Y.; Li, H.H.; Zhang, H.J. Risk-Averse Two-Stage Stochastic Minimum Cost Consensus Models with Asymmetric Adjustment Cost. *Group Decis. Negot.* **2022**, *31*, 261–291. [[CrossRef](#)]
26. Soyster, A.L. Technical Note—Convex Programming with Set-Inclusive Constraints and Applications to Inexact Linear Programming. *Oper. Res.* **1973**, *21*, 1154–1157. [[CrossRef](#)]
27. Ben-Tal, A.; Nemirovski, A. Robust solutions of uncertain linear programs. *Oper. Res. Lett.* **1999**, *88*, 411–424. [[CrossRef](#)]
28. Ben-Tal, A.; Nemirovski, A. Robust Convex Optimization. *Math. Oper. Res.* **1998**, *23*, 769–805. [[CrossRef](#)]
29. Bertsimas, D.; Sim, M. Robust discrete optimization and network flows. *Math. Program.* **2003**, *98*, 49–71. [[CrossRef](#)]
30. Bertsimas, D.; Sim, M. The Price of Robustness. *Oper. Res.* **2004**, *52*, 35–53. [[CrossRef](#)]
31. Ji, Y.; Jin, X.W.; Xu, Z.S.; Qu, S.J. A mixed 0-1 programming approach for multiple attribute strategic weight manipulation based on uncertainty theory. *J. Intell. Fuzzy Syst.* **2021**, *41*, 6739–6754. [[CrossRef](#)]
32. Qu, S.J.; Li, Y.M.; Ji, Y. The mixed integer robust maximum expert consensus models for large-scale GDM under uncertainty circumstances. *Appl. Soft Comput.* **2021**, *107*, 107369. [[CrossRef](#)]
33. Zhang, H.J.; Ji, Y.; Qu, S.J.; Li, H.H.; Huang, R.P. The robust minimum cost consensus model with risk aversion. *Inf. Sci.* **2022**, *587*, 283–299. [[CrossRef](#)]
34. Han, Y.; Qu, S.J.; Wu, Z.; Huang, R.P. Robust consensus models based on minimum cost with an application to marketing plan. *J. Intell. Fuzzy Syst.* **2019**, *37*, 5655–5668. [[CrossRef](#)]
35. Li, C.N.; Guo, T.Y.; Chen, Y. Robust Emission Reduction Strategies under Cap-and-Trade and Demand Uncertainty. *Sustainability* **2022**, *14*, 13445. [[CrossRef](#)]
36. Qu, S.J.; Wei, J.P.; Wang, Q.H.; Li, Y.M.; Jin, X.W.; Chaib, L. Robust minimum cost consensus models with various individual preference scenarios under unit adjustment cost uncertainty. *Inf. Fusion* **2023**, *89*, 510–526. [[CrossRef](#)]
37. Huang, R.P.; Qu, S.J.; Yang, X.G.; Xu, F.M.; Xu, Z.S.; Zhou, W. Sparse portfolio selection with uncertain probability distribution. *Appl. Intell.* **2021**, *51*, 6665–6684. [[CrossRef](#)]
38. Cacador, S.; Dias, J.M.; Godinho, P. Portfolio selection under uncertainty: A new methodology for computing relative-robust solutions. *Int. T. Oper. Res.* **2021**, *28*, 1296–1329. [[CrossRef](#)]
39. Gubu, L.; Rosadi, D.; Abdurakhman. A New Approach for Robust Mean-Variance Portfolio Selection Using Trimmed k-Means Clustering. *Ind. Eng. Manag. Syst.* **2021**, *20*, 782–794. [[CrossRef](#)]
40. Luan, D.Q.; Wang, C.M.; Wu, Z.; Xia, Z.J. Two-Stage Robust Optimization Model for Uncertainty Investment Portfolio Problems. *J. Math.* **2021**, *2021*, 3087066. [[CrossRef](#)]
41. Xu, L.J.; Zhou, Y.J. New Robust Reward-Risk Ratio Models with CVaR and Standard Deviation. *J. Math.* **2022**, *2022*, 8304411. [[CrossRef](#)]
42. Qu, S.J.; Xu, Y.T.; Ji, Y.; Feng, C.; Wei, J.P.; Jiang, S. Data-Driven Robust Data Envelopment Analysis for Evaluating the Carbon Emissions Efficiency of Provinces in China. *Sustainability* **2022**, *14*, 13318. [[CrossRef](#)]

43. Qu, S.J.; Feng, C.; Jiang, S.; Wei, J.P.; Xu, Y.T. Data-Driven Robust DEA Models for Measuring Operational Efficiency of Endowment Insurance System of Different Provinces in China. *Sustainability* **2022**, *14*, 9954. [[CrossRef](#)]
44. Ji, Y.; Du, J.H.; Han, X.Y.; Wu, X.Q.; Huang, R.P.; Wang, S.L.; Liu, Z.M. A mixed integer robust programming model for two-echelon inventory routing problem of perishable products. *Physica A* **2020**, *548*, 124481. [[CrossRef](#)]
45. Liu, Z.M.; Qu, S.J.; Raza, H.; Wu, Z.; Qu, D.Q.; Du, J.H. Two-stage mean-risk stochastic mixed integer optimization model for location-allocation problems under uncertain environment. *J. Ind. Manag. Optim.* **2021**, *17*, 2783–2804. [[CrossRef](#)]
46. Liu, H.R.; Qu, S.J.; Li, R.J.; Razaa, H. Bi-objective robust project scheduling with resource constraints and flexible activity execution lists. *Comput. Ind. Eng.* **2021**, *156*, 107288. [[CrossRef](#)]
47. Kumar Tarei, P.; Kumar, G.; Ramkumar, M. A Mean-Variance robust model to minimize operational risk and supply chain cost under aleatory uncertainty: A real-life case application in petroleum supply chain. *Comput. Ind. Eng.* **2022**, *166*, 107949. [[CrossRef](#)]
48. Savoji, H.; Mousavi, S.M.; Antucheviciene, J.; Pavlovskis, M. A Robust Possibilistic Bi-Objective Mixed Integer Model for Green Biofuel Supply Chain Design under Uncertain Conditions. *Sustainability* **2022**, *14*, 13675. [[CrossRef](#)]
49. Kaoud, E.; Abdel-Aal, M.A.M.; Sakaguchi, T.; Uchiyama, N. Robust Optimization for a Bi-Objective Green Closed-Loop Supply Chain with Heterogeneous Transportation System and Presorting Consideration. *Sustainability* **2022**, *14*, 10281. [[CrossRef](#)]
50. Sun, H.P.; Li, Y.C.; Zhang, J.H. Collaboration-based reliable optimal casualty evacuation network design for large-scale emergency preparedness. *Socio. Econ. Plan. Sci.* **2021**, *81*, 101192. [[CrossRef](#)]
51. Zhang, J.H.; Liu, H.Y.; Yu, G.D.; Ruan, J.H.; Chan, F.T.S. A three-stage and multi-objective stochastic programming model to improve the sustainable rescue ability by considering secondary disasters in emergency logistics. *Comput. Ind. Eng.* **2019**, *135*, 1145–1154. [[CrossRef](#)]
52. Zhang, Y.W.; Li, Z.P.; Jiao, P.B.; Zhu, S. Two-stage stochastic programming approach for limited medical reserves allocation under uncertainties. *Complex Intell. Syst.* **2021**, *7*, 3003–3013. [[CrossRef](#)]
53. Jamali, A.; Ranjbar, A.; Heydari, J.; Nayeri, S. A multi-objective stochastic programming model to configure a sustainable humanitarian logistics considering deprivation cost and patient severity. *Ann. Oper. Res.* **2021**, *2021*, 1–35. [[CrossRef](#)]
54. Yin, X.C.; Büyüktaktakın, İ.E. A multi-stage stochastic programming approach to epidemic resource allocation with equity considerations. *Health Care Manag. Sci.* **2021**, *24*, 597–622. [[CrossRef](#)]
55. Zhang, Z.; Li, Z.L. Consensus-based TOPSIS-Sort-B for multi-criteria sorting in the context of group decision-making. *Ann. Oper. Res.* **2022**, *2022*, 1–28. [[CrossRef](#)]
56. Gai, T.T.; Cao, M.S.; Chiclana, F.; Zhang, Z.; Dong, Y.C.; Herrera-Viedma, E.; Wu, J. Consensus-trust Driven Bidirectional Feedback Mechanism for Improving Consensus in Social Network Large-group Decision Making. *Group Decis. Negot.* **2022**, *2022*, 1–30. [[CrossRef](#)]
57. Zhang, Z.; Li, Z.L. Personalized Individual Semantics-Based Consistency Control and Consensus Reaching in Linguistic Group Decision Making. *IEEE Trans. Syst. Man Cybern. Syst.* **2022**, *52*, 5623–5635. [[CrossRef](#)]
58. Gao, Y.; Zhang, Z. Consensus reaching with non-cooperative behavior management for personalized individual semantics-based social network group decision making. *J. Oper. Res. Soc.* **2021**, *2021*, 1–18. [[CrossRef](#)]
59. Pamucar, D.; Torkayesh, A.E.; Biswas, S. Supplier selection in healthcare supply chain management during the COVID-19 pandemic: A novel fuzzy rough decision-making approach. *Ann. Oper. Res.* **2022**, *2022*, 1–43. [[CrossRef](#)]
60. Biswas, S.; Pamucar, D.; Bozanic, D.; Halder, B. A New Spherical Fuzzy LBWA-MULTIMOOSRAL Framework: Application in Evaluation of Leanness of MSMEs in India. *Math. Probl. Eng.* **2022**, 5480848. [[CrossRef](#)]
61. Qu, S.J.; Shu, L.L.; Yao, J.Y. Optimal pricing and service level in supply chain considering misreport behavior and fairness concern. *Comput. Ind. Eng.* **2022**, *174*, 108759. [[CrossRef](#)]
62. Qu, S.J.; Xu, L.; Mangla, S.K.; Chan, F.T.S.; Zhu, J.L.; Arisian, S. Matchmaking in reward-based crowdfunding platforms: A hybrid machine learning approach. *Int. J. Prod. Res.* **2022**, *2022*, 1–21. [[CrossRef](#)]

Disclaimer/Publisher’s Note: The statements, opinions and data contained in all publications are solely those of the individual author(s) and contributor(s) and not of MDPI and/or the editor(s). MDPI and/or the editor(s) disclaim responsibility for any injury to people or property resulting from any ideas, methods, instructions or products referred to in the content.